78 *Biochemistry* **2010,** *49,* 78–83
DOI: 10.1021/bi901695p

BIOCHEMISTRY
including biophysical chemistry & molecular biology
Article

Variations at the Semiconserved Glycine in the IQ Domain Consensus Sequence Have a Major Impact on Ca^{2+}-Dependent Switching in Calmodulin−IQ Domain Complexes[†]

D. J. Black and Anthony Persechini*

Division of Molecular Biology and Biochemistry, University of Missouri—Kansas City, Kansas City, Missouri 64110-2499

Received September 29, 2009; Revised Manuscript Received December 1, 2009

ABSTRACT: We have replaced the semiconserved Gly in the IQ domain consensus sequence with Ala, Arg, or Met in a reference sequence and determined how this affects its complexes with calmodulin. The K_d for the Ca^{2+}-free reference complex is 2.4 ± 0.3 μM. The Ala and Arg replacements increase this to 5.4 ± 0.4 and 6.2 ± 0.5 μM, while the Met increases it to 26.4 ± 2.5 μM. When Ca^{2+} is bound to both calmodulin lobes, the K_d for the reference complex is not significantly affected, but the K_d for the Ala variant decreases to 0.9 ± 0.04 μM, and the values for the Arg and Met variants decrease to 0.4 ± 0.03 μM. Using mutant calmodulins, we defined the effect of Ca^{2+} binding to each lobe, with the C-terminal preceding the N-terminal (C→N) or vice versa (N→C). In the C→N order the first step increases the reference K_d ~5-fold, while it decreases the values for the variants ~2- to ~10-fold. The second step decreases the K_d values for the all of the complexes ~5-fold, suggesting that the N-terminal lobe does not interact with the semiconserved position after the first step. In the N→C order the first step increases the K_d values for the reference complex and Met and Ala variants ~15- to ~200-fold but does not affect the value for the Arg variant. The second step decreases the K_d values for the reference and Arg variant ~10- and ~15-fold and the Ala and Met variants ~2000-fold. Thus, both steps in the N→C order are sensitive to variations at the semiconserved position, while only the first is in the C→N order. Due to energy coupling, this order is followed under equilibrium conditions.

The Ca^{2+}-binding protein calmodulin (CaM)[1] plays a key role in the orchestration of cell function because it interacts with a large number of different proteins and modulates their activities. These interactions are to varying extents controlled by the intracellular concentration of free Ca^{2+}, which is detected via the two pairs of EF hand Ca^{2+}-binding sites in CaM. Each pair of sites comprises a globular lobe, and the two lobes are tethered by a flexible linker (*1*−*3*). Due to cooperativity within each EF hand pair, $(Ca^{2+})_2$-CaM, with Ca^{2+} bound to the N- or C-lobe, and $(Ca^{2+})_4$-CaM are the major Ca^{2+}-bound species produced (*4*). Although there is no general CaM-binding consensus sequence, a number of proteins including neuromodulin and PEP19, unconventional myosins, several ion channels, and modulators of small G-proteins bind CaM through IQ domains, which have the consensus sequence [I,L,V]Q*xxx*R[G,*x*]*xxx*[R,K] (*5*−*8*). Depending upon their sequences, these domains interact with CaM in its Ca^{2+}-free and Ca^{2+}-bound forms with varying degrees of preference, so as to generate a range of Ca^{2+}-dependent switching behaviors (*7*). We have begun to analyze Ca^{2+}-dependent switching in CaM−IQ domain complexes in order to identify and categorize different types of switching and determine how they are encoded in IQ domain sequences.

Structural and biophysical studies suggest that variable interactions with the CaM N-lobe are a likely contributor to variability in Ca^{2+}-dependent switching. These indicate that Ca^{2+}-free CaM forms two types of complexes with IQ domains. One is compact, with the CaM N-lobe bound to a site that includes the semiconserved Gly position in the IQ domain consensus sequence (*9*−*11*). In the other the N-lobe extends into the solvent and has few interactions with the IQ domain (*10*, *11*). Formation of the compact conformation seems to require a small amino acid at the semiconserved position (*10*, *11*). In these complexes the IQ domain is α-helical in conformation, with the CaM C-lobe bound in a parallel orientation to a site that includes the "IQ" amino acid pair (*9*−*11*). In the structures that have so far been determined for Ca^{2+}-saturated CaM−IQ domain complexes, the CaM-binding sequence is also α-helical, and the C-lobe is bound in a parallel orientation to the same site, although interacting differently with the IQ amino acid pair (*12*, *13*). However, in these structures the N-lobe binds to a site on the opposite side of the C-lobe from the site it occupies in the Ca^{2+}-free complexes (*12*, *13*). Based on these observations, variations at the semiconserved Gly in the IQ domain consensus sequence would be expected to influence the distribution of the N-lobe between different binding modes in Ca^{2+}-free and probably also one or both intermediate Ca^{2+}-bound complexes, thereby affecting Ca^{2+}-dependent switching. In the Ca^{2+}-saturated complex variations at this position would not be expected to directly affect interactions with the N-lobe.

We have recently investigated how Ca^{2+}-dependent switching in a reference CaM−IQ domain complex is affected when the Gly

[†]This work was supported by NIH Grant DK53863 to A.P.

*To whom correspondence should be addressed. Tel: 816-235-6076. Fax: 816-235-5595. E-mail: Persechinia@umkc.edu.

[1]Abbreviations: CaM, calmodulin; C-lobe and N-lobe, C-terminal and N-terminal lobes in CaM; B_{IQ}, fluorescent reporter containing an IQ domain sequence derived from neuromodulin; $B_{IQ}G^6A$, $B_{IQ}G^6R$, and $B_{IQ}G^6M$, variants of B_{IQ} with replacements A, R, and M for the G at the position 6; N_xCCaM (N_xC), mutant CaM with E31A and E67A replacements; NC_xCaM (NC_x), mutant CaM with E104A and E140A replacements; N→C Ca^{2+}-binding order, Ca^{2+} is bound to the C-lobe before the N-lobe; C→N Ca^{2+}-binding order, Ca^{2+} is bound to the N-lobe before the C-lobe; BAPTA, 1,2-bis(2-aminophenoxy)ethane-*N*,*N*,*N*′,*N*′-tetraacetic acid; dibromo-BAPTA, 1,2-bis(2-amino-5,5′-dibromophenoxy)ethane-*N*,*N*,*N*′,*N*′-tetraacetic acid; TPEN, tetrakis(2-pyridylmethyl)ethylenediamine.

 Published on Web 12/02/2009

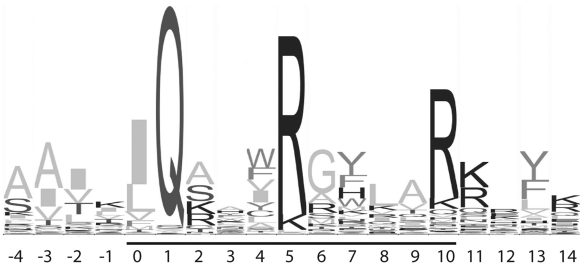

	-4	-3	-2	-1	0	1	2	3	4	5	6	7	8	9	10	11	12	13	14
B_{IQ}	A	A	T	K	I	Q	A	A	F	R	G	H	I	T	R	K	K	L	K
$B_{IQ}G^6A$	A	A	T	K	I	Q	A	A	F	R	A	H	I	T	R	K	K	L	K
$B_{IQ}G^6R$	A	A	T	K	I	Q	A	A	F	R	R	H	I	T	R	K	K	L	K
$B_{IQ}G^6M$	A	A	T	K	I	Q	A	A	F	R	M	H	I	T	R	K	K	L	K

FIGURE 1: IQ domain insert sequences in the reference and variant reporter constructs. The insert sequences are numbered in relation to the first residue (0) in the 11-residue canonical IQ domain consensus sequence: [I,L,V]QxxxR[G,x]xxx[R,K]. A logo representation of the hidden Markov model profile derived from ~3000 IQ domain sequences in the Pfam-A database is shown (*23*, *24*). The canonical consensus region is underlined. Each position is represented by a stack of one-letter amino acid symbols. The total height of a stack is an indication of how well conserved that position is, and the height of each symbol in a stack is an indication of its relative frequency. The sequences listed below the logo representation correspond to the inserts in the reference (B_{IQ}) and variant CaM-binding reporter constructs (*15*−*17*). The complete inserts include the additional C-terminal amino acid sequence, DEKKGA, which is not shown.

at the semiconserved position is replaced with the Lys variation in the PEP19 sequence (*14*). Our results suggest that the presence or absence of the Gly defines two major classes of CaM−IQ domain complexes with distinct switching behaviors (*14*). To confirm and extend this initial finding, we have investigated the effects of Ala, Arg, and Met variations. To different extents they all stabilize the complex with Ca^{2+}-saturated CaM, or CaM with Ca^{2+}-bound only to its C-lobe, and destabilize the complex with Ca^{2+}-free CaM. However, when Ca^{2+} is bound only to the N-lobe, Met and Ala are destabilizing while Arg is stabilizing. Although our results confirm that the presence or absence of the semiconserved Gly defines two major functional classes, they also indicate that different variants produce distinct Ca^{2+}-dependent switching behaviors.

MATERIALS AND METHODS

B_{IQ}, a fluorescent reporter that binds CaM via an IQ domain sequence derived from neuromodulin, has been described elsewhere (*15*−*17*). The CaM-binding sequence in this construct is inserted between cyan and yellow variants of green fluorescence protein. When CaM is bound, fluorescence resonance transfer (FRET) from the cyan donor to the yellow acceptor is decreased (*15*−*17*). The B_{IQ} construct and intact neuromodulin have previously been shown to bind CaM with similar affinities (*15*). The insert sequences in the B_{IQ} reference construct and variants with the indicated amino acid replacements at position 6 are listed in Figure 1. Two mutant CaMs were employed to determine the effects of Ca^{2+} binding to only the N-ter or C-ter EF hand pair: N_xCCaM (N_xC), in which Ca^{2+} ligands at positions 31 and 67 in the N-lobe pair have been replaced with alanines, and NC_xCaM (NC_x), in which the homologous ligands at positions 104 and 140 in the C-lobe have been replaced (*15*). We have previously established that EF hand pairs disabled in this manner do not bind significant amounts of Ca^{2+} under our experimental conditions (*15*). Fluorescent reporters and native and mutant CaMs were expressed and purified as described in detail previously (*18*−*20*).

Fluorescence Measurements and Analysis of Fluorescence Data. A Photon Technologies International (Monmouth Junction, NJ) QM-1 fluorometer operated in photon-counting mode was used for all fluorescence measurements. Monochromator excitation and emission bandwidths were ~2.5 nm. All experiments were performed at 23 °C. The standard experimental buffer contained 25 mM Tris (pH 7.5), 100 mM KCl, 100 μg/mL BSA, 25 μM TPEN, and other components as specified in the text or captions. Nominally Ca^{2+}-free conditions were produced by including 3 mM BAPTA. Saturation of functional Ca^{2+} binding sites in native or mutant CaMs was in general effected by adding $CaCl_2$ to buffers and CaM stock solutions to produce a final free Ca^{2+} concentration of ~250 μM. Ca^{2+} saturation was verified by adding ~1 mM $CaCl_2$ at the end of each CaM-binding experiment. With complexes expected to have weakened Ca^{2+}-binding affinities due to energy coupling, experiments were performed at a free Ca^{2+} concentration of ~2 mM. Defining the effects of Ca^{2+} binding to each CaM lobe using the N_xCCaM and NC_xCaM mutants requires them to be bound with same affinity as native CaM in the absence of Ca^{2+}. We have previously shown this to be true with the B_{IQ} reference (*15*) and have verified that this holds for the variants investigated here (data not shown).

Decreases in fluorescence emission at 525 nm (430 nm excitation) due to decreases in FRET are directly proportional to fractional saturation of the CaM-binding insert sequences in the reporter constructs. Fractional fluorescence response (FR) is formally defined as $(F_{max} - F)/(F_{max} - F_{min})$, where F corresponds with the fluorescence emission at 525 nm measured after each addition of CaM, and F_{max} and F_{min} correspond respectively with the fluorescence of the CaM-free and CaM-saturated reporter. Apparent K_d values were derived assuming a hyperbolic dependence of FR on the CaM concentration: FR = [CaM]/([CaM] + K_d). This assumption is valid because the 10−100 nM reporter concentrations used in binding experiments are at least 5-fold below the lowest CaM concentrations. Thus, the free and total CaM concentrations are approximately equivalent. Reported K_d values are the means of estimates derived from three to five independent data sets. Errors are expressed as the standard error of the mean (SEM). The difference between two mean values is considered statistically significantly if the p value derived from an unpaired t-test is less than 0.05.

RESULTS

Effects of Amino Variations at the Semiconserved Position on CaM Binding. The semiconserved Gly in the IQ domain consensus sequence (position 6 in Figure 1) is replaced in naturally occurring variants mainly by Ala, Arg, Ser, Met, or Lys (Figure 1). To investigate the functional significance of these variations, we have replaced the Gly in a reference reporter construct (B_{IQ}) with Ala ($B_{IQ}G^6A$), Arg ($B_{IQ}G^6R$), or Met ($B_{IQ}G^6M$) and determined how this affects binding to CaM in its Ca^{2+}-free and various Ca^{2+}-bound states (Figure 1).

Representative data for the B_{IQ} reference and the G^6A, G^6R, and G^6M variants are presented in Figures 2, 3, 4, and 5. The K_d values derived from these and similar data are listed in Table 1. The stability differences ($\Delta\Delta G_B$) between the variant and reference complexes in kilojoules per mole are listed alongside the K_d values. It is easier to discuss changes in stability in terms of these values, rather than fold changes in K_d values. To put these values in perspective, destabilization producing a 2-, 10-, or 100-fold increase in a K_d value corresponds with $\Delta\Delta G_B$ values of 1.7, 5.7,

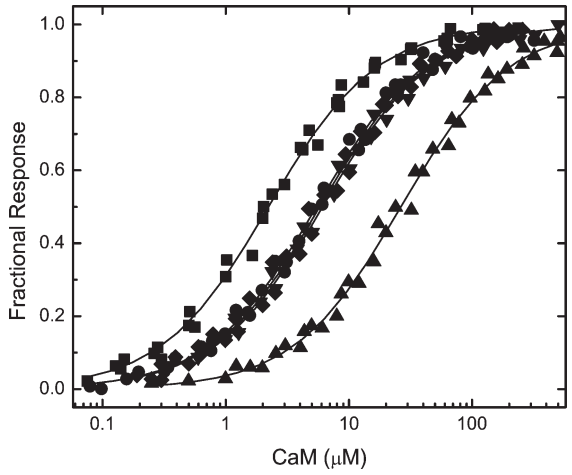

FIGURE 2: Binding of Ca^{2+}-free CaM. Data for binding to the following reporter constructs are presented: B_{IQ} (■), $B_{IQ}G^6A$ (●), $B_{IQ}G^6M$ (▲), $B_{IQ}G^6R$ (▼), and $B_{IQ}G^6K$ (♦). The complete amino acid sequences of the CaM-binding inserts in these reporters are listed in Figure 1. Apparent K_d values were derived from fits of a hyperbolic binding equation to these (solid lines), and similar data are listed in Table 1. Reference and variant reporter concentrations were 10−100 nM. Nominally Ca^{2+}-free conditions were maintained by adding 3 mM BAPTA. The standard experimental buffer contained 25 mM Tris (pH 7.5), 100 mM KCl, 100 μg/mL BSA, 25 μM TPEN, and other components as specified.

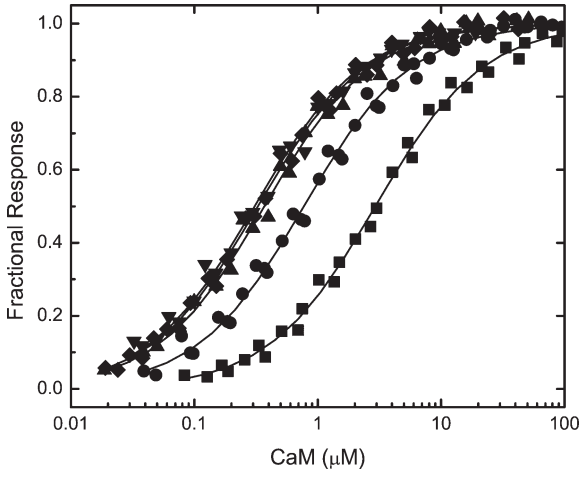

FIGURE 3: Binding of Ca^{2+}-saturated CaM. Ca^{2+} saturation was produced using 0.25−2 mM $CaCl_2$, as detailed in Materials and Methods. Symbols and other details are given in the caption to Figure 2.

or 11.4 kJ/mol. Stabilizations producing decreases by the same factors correspond with negative values with these magnitudes.

The Ala and Arg variations slightly destabilize the Ca^{2+}-free CaM complex, and the Met produces a substantial 5.8 ± 1.0 kJ/mol reduction in stability (Table 1). In contrast, the variations all stabilize the Ca^{2+}-saturated CaM complex, and the Ala, Arg, and Met produce similar $\Delta\Delta G_B$ values of −3.0 ± 0.3, −5.1 ± 0.7, and −5.0 ± 0.8 kJ/mol (Table 1). Using N_xCCaM and NC_xCaM mutants, which have defective N- or C-lobe Ca^{2+}-binding sites, we have defined how the variations affect CaM complexes in which Ca^{2+} is bound only to one lobe or the other. Interestingly, the $\Delta\Delta G_B$ values for the variant complexes with Ca^{2+}-saturated N_xCCaM are essentially identical to those for the Ca^{2+}-saturated complexes with native CaM (Table 1). The Arg variation also has a similar stabilizing effect on the complex with Ca^{2+}-saturated

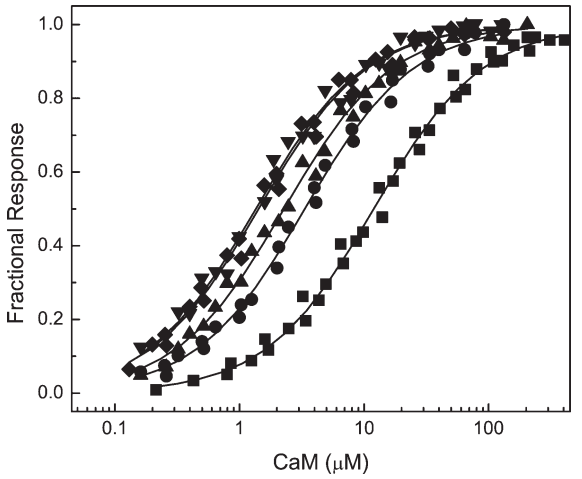

FIGURE 4: Binding of N_xC_2CaM. Saturation of the functional C-terminal EF hand pair in N_xCCaM was produced using 0.25−2 mM $CaCl_2$, as detailed in Materials and Methods. Symbols and additional details are given in Materials and Methods or in the caption to Figure 2.

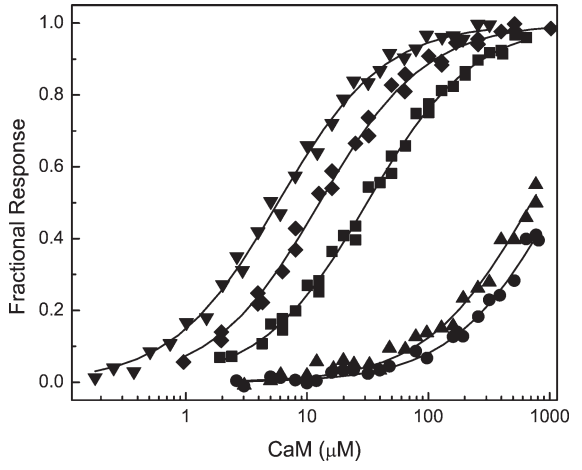

FIGURE 5: Binding of N_2C_xCaM. Saturation of the functional N-terminal EF hand pair in NC_xCaM was produced using 0.25−2 mM $CaCl_2$, as detailed in Materials and Methods. Symbols and additional details are given in Materials and Methods or in the caption to Figure 2.

NC_xCaM. In contrast, the Ala and Met variations significantly destabilize this complex, with essentially identical $\Delta\Delta G_B$ values of 8.9 ± 1.2 and 8.1 ± 1.5 kJ/mol (Table 1).

Effects of Amino Acid Variations on Ca^{2+}-Dependent Switching. As discussed in detail elsewhere, Ca^{2+} binding to a CaM complex can in general be treated as a two-step process (*15*, *21*). In the first step Ca^{2+} binds to the EF hand pair in the C-lobe or N-lobe, and in the second it binds the EF hand pair in the remaining lobe. Thus, there are two possible Ca^{2+}-binding orders: C-lobe before N-lobe (C→N) and vice versa (N→C). Perhaps the most interesting aspect of our results concerns how the amino acid replacements affect the stability changes ($\Delta\Delta G_C$) produced by Ca^{2+} binding, because these govern Ca^{2+}-dependent switching. As detailed in the caption to Table 2, we have calculated $\Delta\Delta G_C$ values from ratios of the K_d values for the Ca^{2+}-free and different Ca^{2+}-bound states of the CaM complexes listed in Table 1. As we have discussed, the K_d values for the two intermediate states were determined using the Ca^{2+}-saturated N_xCCaM and NC_xCaM CaM mutants. The $\Delta\Delta G_C$ values calculated from the N_xC_2/NC and N_2C_2/N_xC_2 K_d ratios correspond

Table 1: Differences between Stabilities of the CaM Complexes with the B_{IQ} Variants and Reference[a]

	NC		N_xC_2		N_2C_x		N_2C_2	
	K_d (μM)	$\Delta\Delta G_B$ (kJ/mol)	K_d (μM)	$\Delta\Delta G_B$ (kJ/mol)	K_d (μM)	$\Delta\Delta G_B$ (kJ/mol)	K_d (μM)	$\Delta\Delta G_B$ (kJ/mol)
B_{IQ}	2.4 ± 0.3		12.7 ± 1.1		31.3 ± 2.7		2.9 ± 0.3	
$B_{IQ}G^6A$	5.4 ± 0.4	2.0 ± 0.3	3.5 ± 0.5	−3.1 ± 0.5	1143.8 ± 101.6	8.9 ± 1.2	0.9 ± 0.04	−3.0 ± 0.3
$B_{IQ}G^6R$	6.2 ± 0.5	2.3 ± 0.4	1.3 ± 0.2	−5.6 ± 1.0	6.2 ± 0.6	−3.9 ± 0.5	0.4 ± 0.03	−5.1 ± 0.7
$B_{IQ}G^6M$	26.4 ± 2.5	5.8 ± 1.0	2.3 ± 0.2	−4.2 ± 0.6	839.8 ± 123.3	8.1 ± 1.5	0.4 ± 0.03	−5.0 ± 0.6

[a]Differences in stability ($\Delta\Delta G_B$) were calculated according to the relation $\Delta\Delta G_B = RT\ln(K_dV/K_dR)$, where K_dR is the K_d value for the reference CaM−B_{IQ} complex and K_dV is the value for a variant complex. The B_{IQ} variants have the indicated amino acid replacements at position 6. The K_d values for the complexes with Ca^{2+}-free and Ca^{2+}-bound CaM are listed alongside the $\Delta\Delta G_B$ values for these complexes. N and C refer to the N- and C-lobes in CaM. A subscript "x" indicates a disabled EF hand pair; a subscript "2" indicates that 2 Ca^{2+} ions are bound. The absence of a subscript indicates a native Ca^{2+}-free EF hand pair.

Table 2: Ca^{2+}-Dependent Changes in Stabilities of CaM Complexes with the B_{IQ} Reference and Variants[a]

	N_xC_2/NC		N_2C_2/N_xC_2		N_2C_x/NC		N_2C_2/N_2C_x		N_2C_2/NC	
construct	K_d ratio	$\Delta\Delta G_C$ (kJ/mol)	K_d ratio	$\Delta\Delta G_C$ (kJ/mol)	K_d ratio	$\Delta\Delta G_C$ (kJ/mol)	K_d ratio ($\times10^{-2}$)	$\Delta\Delta G_C$ (kJ/mol)	K_d ratio	$\Delta\Delta G_C$ (kJ/mol)
B_{IQ}	5.4 ± 0.8	4.1 ± 0.6	0.2 ± 0.03	−3.5 ± 0.5	14.1 ± 1.9	6.5 ± 0.9	9.0 ± 1.2	−5.8 ± 0.8	1.3 ± 0.2	0.7 ± 0.1
$B_{IQ}G^6A$	0.6 ± 0.1	−1.1 ± 0.2	0.2 ± 0.03	−3.5 ± 0.5	207.3 ± 18.1	13.1 ± 1.3	0.07 ± 0.06	−17.6 ± 1.4	0.16 ± 0.02	−4.6 ± 0.4
$B_{IQ}G^6R$	0.2 ± 0.04	−3.8 ± 0.7	0.3 ± 0.05	−3.2 ± 0.6	1.0 ± 0.1	0.03 ± 0.003	6.0 ± 0.6	−7.0 ± 0.8	0.06 ± 0.007	−7.0 ± 0.8
$B_{IQ}G^6M$	0.1 ± 0.02	−6.0 ± 0.7	0.2 ± 0.02	−4.1 ± 0.5	31.9 ± 5.6	8.5 ± 1.5	0.04 ± 0.07	−18.9 ± 3.2	0.01 ± 0.002	−10.5 ± 1.4

[a]Ca^{2+}-dependent changes in stability ($\Delta\Delta G_C$) were calculated according to the relation $\Delta\Delta G_C = RT\ln(K_d'/K_d)$, where K_d' and K_d are the K_d values for a B_{IQ} reference or variant complex with CaM in two different Ca^{2+}-bound states (Table 1). K_d'/K_d ratios for the complexes with CaM in the indicated states are listed alongside the $\Delta\Delta G_C$ values derived from them. N and C refer to the N-ter and C-ter EF hand pairs in CaM. A subscript "x" indicates a disabled EF hand pair, and a subscript "2" indicates that 2 Ca^{2+} ions are bound. The absence of a subscript indicates a native Ca^{2+}-free EF hand pair. The B_{IQ} variants have the indicated amino acid replacements at position 6.

with the first and second Ca^{2+}-binding steps in the C→N Ca^{2+}-binding order. The values calculated from the N_2C_x/NC and N_2C_2/N_2C_x K_d ratios correspond with the first and second steps in the N→C binding order, and those calculated from the N_2C_2/NC K_d ratios are a measure of the overall change in stability produced when Ca^{2+} has occupied both CaM lobes (see Table 2).

The first step in the C→N Ca^{2+}-binding order decreases the stability of the B_{IQ} reference complex, with a $\Delta\Delta G_C$ value of 4.1 ± 0.6 kJ/mol. This step significantly increases the stabilities of the Arg and Met variant complexes, with $\Delta\Delta G_C$ values of −3.8 ± 0.7 and −6.0 ± 0.7 kJ/mol, but only slightly stabilizes the Ala variant, with a $\Delta\Delta G_C$ value of −1.1 ± 0.2 kJ/mol. Surprisingly, the second Ca^{2+}-binding step increases the stabilities of the B_{IQ} reference complex and the variants to the same extent, with $\Delta\Delta G_C$ values of ∼−3.5 kJ/mol (Table 2). This suggests that the N-lobe does not interact significantly with the semiconserved position in either the intermediate or final states in this Ca^{2+}-binding order, although these are both stabilized in the variant complexes (Table 1). This implies that stabilization involves only the C-lobe.

The first step in the N→C Ca^{2+}-binding order also decreases the stability of the B_{IQ} reference complex, with a $\Delta\Delta G_C$ value of 6.5 ± 0.9 kJ/mol, and it substantially destabilizes the Ala and Met variant complexes, with $\Delta\Delta G_C$ values of 13.1 ± 1.3 and 8.5 ± 1.5 kJ/mol. However, it has no effect on the stability of the Arg variant complex. The second step increases the stabilities of the reference and Arg variant complexes similarly, with $\Delta\Delta G_C$ values of −5.8 ± 0.8 and −7.0 ± 0.8 kJ/mol. It dramatically stabilizes the Ala and Met variant complexes, with essentially identical $\Delta\Delta G_C$ values of −17.6 ± 1.4 and −18.9 ± 3.2 kJ/mol. This suggests that the Ala and Met variant complexes with CaM are in a similar destabilizing conformation in the intermediate Ca^{2+}-bound state.

Only the C→N Ca^{2+}-Binding Order Is Significant under Equilibrium Conditions. The ratio of the apparent K_d values for the first Ca^{2+}-binding step in the C→N and N→C Ca^{2+}-binding orders, i.e., binding initially to the C-lobe versus the N-lobe, determines the distribution between the two pathways under equilibrium conditions. Although we have not made any Ca^{2+}-binding measurements here, due to thermodynamic equivalencies this ratio can be derived from the $\Delta\Delta G_C$ value for the first step in each binding order, as discussed in detail elsewhere (*15*). As reported previously, the ratio for the B_{IQ} reference complex is ∼7 (*15*). Hence, the C→N Ca^{2+}-binding order is followed ∼90% of the time. We have derived significantly larger values of ∼115, ∼14, and ∼126 for the Ala, Arg, and Met variant complexes. Thus, under equilibrium conditions the C→N Ca^{2+}-binding order appears to be followed almost exclusively.

DISCUSSION

Replacing the semiconserved Gly in the consensus IQ domain with Ala, Arg, or Met, which are prominent natural variants, destabilizes the Ca^{2+}-free CaM−B_{IQ} complex and stabilizes the Ca^{2+}-saturated complex (Table 1). Stabilization appears to principally involve the Ca^{2+}-bound C-lobe, because it remains the same whether or not Ca^{2+} is bound to the N-lobe (Table 1). In contrast, when Ca^{2+} is bound to the N-lobe, the effects of the amino acid variations depend upon the status of the C-lobe (Table 1). Consequently, both steps in the N→C Ca^{2+}-binding order are sensitive to variation at the semiconserved position, while only the first step appears to be in the alternative C→N order. As addressed in Results, due to energy coupling the N→C order does not play a significant role under equilibrium conditions and will not be discussed in detail here. However, as seen with the reference CaM−B_{IQ} complex, this binding order may play a significant role under transient conditions, or in a ternary

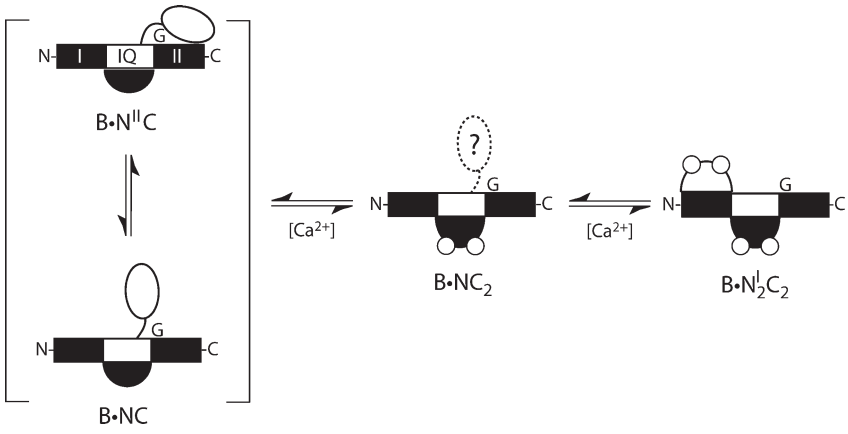

FIGURE 6: A schematic representation of the conformational states of the C-lobe and N-lobe in the C→N Ca^{2+} binding order. Bound Ca^{2+} ions are indicated by small empty circles. The CaM-binding sequence is depicted as a rectangle containing three separate binding sites (I, IQ, and II). The semiconserved Gly position is indicated by a "G". Structural data suggest that in the Ca^{2+}-free complex the N-lobe (empty ellipse) either interacts with site II ($B \cdot N^{II}C$) or is in an extended conformation (B·NC), while in the Ca^{2+}-saturated complex the N-lobe interacts with site I ($B \cdot N_2^{I}C_2$) (*9*−*13*). These data further suggest that the C-lobe (filled semicircle) interacts only with the IQ site. The N-lobe is tentatively depicted in the extended conformation in the intermediate Ca^{2+}-bound state ($B \cdot NC_2$), although it could potentially interact with site I. Only the C→N Ca^{2+} binding order is considered because the alternative N→C order is not relevant under equilibrium conditions (see text).

complex, where additional binding sites for the CaM lobes come into play (*21*). Investigations of the effects of amino acid variations at the semiconserved position under transient conditions are ongoing.

Variations at the Semiconserved Position Affect Interactions with the N-Lobe. High-resolution structures have been determined for complexes between Ca^{2+}-free CaM or myosin light chains and myosin V IQ domains (*9*−*11*) and for Ca^{2+}-saturated CaM bound to the $Ca_v1.2$ IQ domain (*12*, *13*). These indicate that in the presence and absence of Ca^{2+} the N-lobe binds the IQ domain on opposite sides of the C-lobe. They also indicate that in the absence of Ca^{2+} the N-lobe can adopt an extended conformation, in which it has few interactions with the IQ domain (*9*−*11*). Therefore, the N-lobe appears to have at least three distinct conformational states: extended and bound to a site on one side of the C-lobe or the other. In contrast, there appears to be only one binding site for the C-lobe, which occupies it in the same orientation in the presence and absence of Ca^{2+} (*9*, *10*, *12*, *13*). The IQ domain is α-helical in all of the structures that have been determined (*9*, *10*, *12*, *13*). Structural data and fluorescence energy transfer experiments with labeled CaM and IQ domain peptides indicate that in the absence of Ca^{2+} variations at the semiconserved Gly position affect the equilibrium between the extended and bound conformations of the N-lobe (*9*−*11*).

A Role for Alternative N-Lobe Conformations in Ca^{2+}-Dependent Switching. To evaluate our results in terms of these recent structural insights, we shall refer to the schematic presented in Figure 6. The α-helical CaM-binding sequence is represented by a rectangle. The C-lobe binding site, which contains the IQ amino acid pair, is labeled "IQ", and the alternative binding sites for the N-lobe, suggested by structures for the Ca^{2+}-saturated and Ca^{2+}-free complexes, are respectively labeled "I" and "II". Small open circles indicate bound Ca^{2+} ions. The N-lobe is represented by an empty ellipse when Ca^{2+}-free and an empty semicircle when Ca^{2+}-bound to indicate that its hydrophobic cleft is closed in the former and open in the latter, where it is available to interact with the CaM-binding sequence (*9*, *10*, *12*, *13*). The C-lobe is represented by similar filled semicircular shapes in both states because it interacts with the IQ site via a partially open hydrophobic cleft when Ca^{2+}-free and a fully open cleft when Ca^{2+}-bound (*9*, *10*, *12*, *13*).

The standard IQ domain consensus sequence encompasses what we have termed sites II and IQ. It appears that it should be extended to encompass site I. Consistent with this, the sequence profile presented in Figure 1 indicates that there are semi-conserved residues in this region. However, if site I binds only a Ca^{2+}-bound N-lobe, it is likely to be degenerate. There is no clear consensus among the ~100 known amino sequences that bind Ca^{2+}-saturated CaM, although all contain combinations of the hydrophobic and basic amino acids. The schematic representation in Figure 6 is not meant to imply rigid boundaries between the different binding sites. However, structural data clearly place the "IQ" amino acid pair in the C-lobe binding site and the semiconserved Gly position (indicated by a "G") in site II, where it affects interactions with the N-lobe in Ca^{2+}-free complexes (*9*, *10*, *12*, *13*).

In the Ca^{2+}-free complex the C-lobe is bound to the IQ site, and the N-lobe is depicted in an equilibrium between a bound state, where it interacts with site II, and an extended state (Figure 6). Based on the available structures and interaction studies performed using CaM−peptide complexes, an Arg or Met variation at the semiconserved position is expected to favor the extended state, while an Ala, or the semiconserved Gly itself, is expected to favor the bound state (*10*). Consistent with this, the Met variation significantly destabilizes the Ca^{2+}-free complex, with a $\Delta\Delta G_B$ value of ~6 kJ/mol, and the Ala variation produces a relatively small ~2 kJ/mol destabilization. However, the similar effect of the Ala and Arg variations [a Lys is also similar (*14*)] is puzzling, since the Arg should favor an extended N-lobe conformation (*10*). A compensatory electrostatic interaction(s) with CaM, which is rich in acidic amino acids, may account for this. Given an α-helical CaM-binding sequence, any substitution for the semiconserved Gly is likely to result in helix stabilization. This could offset decreases in stability due to reduced N-lobe binding. Although an equilibrium between bound and extended N-lobe conformations in the absence of Ca^{2+} is consistent with our results, further study will be required to determine precisely how it is affected by variations at the semiconserved position.

A role for N-lobe binding to alternative sites is well supported when we consider the stability changes in the C→N Ca^{2+}-binding order. The Ala, Arg, and Met variations have no effect on the $\Delta\Delta G_C$ value for the second Ca^{2+}-binding step, although each

stabilizes the intermediate and final states to the same extent (Tables 1 and 2). This suggests that that the N-lobe does not interact significantly with the semiconserved position after the first Ca^{2+}-binding step. As depicted in Figure 6, structural data suggest that the N-lobe is bound to site I in the Ca^{2+}-saturated complex (*12*, *13*). It does not interact with the semiconserved position in these structures (*12*, *13*). This is clearly consistent with a lack of interaction in the intermediate and Ca^{2+}-saturated states. Otherwise, it would be difficult to reconcile the identical effects of the amino acid variations on the stabilities of the two states (Table 1). The N-lobe is tentatively depicted in an extended conformation in the intermediate state (Figure 6). It could also interact with site I in this state, although this interaction would be expected to be weaker than in the final state, because Ca^{2+} binding to the N-lobe substantially increases stability (Table 2).

What Directs the N-Lobe to Its Alternative Binding Sites? An interesting question raised by the preceding discussion is how the N-lobe is directed to site I or II. Structural data suggest that a change in the orientation of the bound C-lobe is not a factor (*9*, *10*, *12*, *13*). On the other hand, the structures that have been determined for Ca^{2+}-saturated CaM bound to several different non-IQ domain sequences strongly suggest that the orientation of the C-lobe determines where the N-lobe binds (*22*). Given the parallel orientation of the C-lobe in the structures that have been determined for Ca^{2+}-saturated CaM−IQ domain complexes, binding of the N-lobe to site I is expected (*12*, *13*). Although the determinants establishing this relationship are not known, they are apparently affected when Ca^{2+} is removed from the C-lobe, since the N-lobe then appears to be directed to site II (*9*). The substantial destabilizing effect of the Ala and Met variations when Ca^{2+} is bound only to the N-lobe suggests that this lobe forms an unfavorable interaction with site II, perhaps because it is restricted from interacting favorably with site I (Table 1). This interaction may involve contacts between the open hydrophobic cleft in the Ca^{2+}-bound N-lobe and the semiconserved position, since it is promoted by a Met or Ala and prevented by an Arg (Table 1).

REFERENCES

1. Persechini, A., and Kretsinger, R. H. (1988) The central helix of calmodulin functions as a flexible tether. *J. Biol. Chem. 263*, 12175–12178.
2. Persechini, A., Moncrief, N. D., and Kretsinger, R. H. (1989) The EF-hand family of calcium-modulated proteins. *Trends Neurosci. 12*, 462–467.
3. Babu, Y. S., Bugg, C. E., and Cook, W. J. (1988) Structure of calmodulin refined at 2.2 Å resolution. *J. Mol. Biol. 204*, 191–204.
4. Forsén, S., Vogel, H. J., and Drakenberg, T. (1986) Biophysical studies of calmodulin, in Calcium and Cell Function (Cheung, W. Y., Ed.) pp 113−157, Academic Press, New York.
5. Mooseker, M. S., and Cheney, R. E. (1995) Unconventional myosins. *Annu. Rev. Cell Dev. Biol. 11*, 633–675.
6. Yus-Najera, E., Santana-Castro, I., and Villarroel, A. (2002) The identification and characterization of a noncontinuous calmodulin-binding site in noninactivating voltage-dependent KCNQ potassium channels. *J. Biol. Chem. 277*, 28545–28553.
7. Jurado, L. A., Chockalingam, P. S., and Jarrett, H. W. (1999) Apocalmodulin. *Physiol. Rev. 79*, 661–682.
8. Bahler, M., and Rhoads, A. (2002) Calmodulin signaling via the IQ motif. *FEBS Lett. 513*, 107–113.
9. Houdusse, A., Gaucher, J. F., Krementsova, E., Mui, S., Trybus, K. M., and Cohen, C. (2006) Crystal structure of apo-calmodulin bound to the first two IQ motifs of myosin V reveals essential recognition features. *Proc. Natl. Acad. Sci. U.S.A. 103*, 19326–19331.
10. Terrak, M., Rebowski, G., Lu, R. C., Grabarek, Z., and Dominguez, R. (2005) Structure of the light chain-binding domain of myosin V. *Proc. Natl. Acad. Sci. U.S.A. 102*, 12718–12723.
11. Terrak, M., Wu, G. M., Stafford, W. F., Lu, R. C., and Dominguez, R. (2003) Two distinct myosin light chain structures are induced by specific variations within the bound IQ motifs—functional implications. *EMBO J. 22*, 362–371.
12. Fallon, J. L., Halling, D. B., Hamilton, S. L., and Quiocho, F. A. (2005) Structure of calmodulin bound to the hydrophobic IQ domain of the cardiac Ca(v)1.2 calcium channel. *Structure 13*, 1881–1886.
13. Van Petegem, F., Chatelain, F. C., and Minor, D. L. (2005) Insights into voltage-gated calcium channel regulation from the structure of the Ca(V)1.2 IQ domain-Ca^{2+}/calmodulin complex. *Nat. Struct. Mol. Biol. 12*, 1108–1115.
14. Black, D. J., LaMartina, D., and Persechini, A. (2009) The IQ domains in neuromodulin and PEP19 represent two major functional classes. *Biochemistry 48*, 11766–11772.
15. Black, D. J., Leonard, J., and Persechini, A. (2006) Biphasic Ca^{2+}-dependent switching in a calmodulin-IQ domain complex. *Biochemistry 45*, 6987–6995.
16. Persechini, A., and Cronk, B. (1999) The relationship between the free concentrations of Ca^{2+} and Ca^{2+}-calmodulin in intact cells. *J. Biol. Chem. 274*, 6827–6830.
17. Persechini, A., and Stemmer, P. M. (2002) Calmodulin is a limiting factor in the cell. *Trends Cardiovasc. Med. 12*, 32–37.
18. Persechini, A. (2002) Monitoring the intracellular free Ca(2+)-calmodulin concentration with genetically-encoded fluorescent indicator proteins. *Methods Mol. Biol. 173*, 365–382.
19. Fruen, B. R., Black, D. J., Bloomquist, R. A., Bardy, J. M., Johnson, J. D., Louis, C. F., and Balog, E. M. (2003) Regulation of the RYR1 and RYR2 Ca^{2+} release channel isoforms by Ca^{2+}-insensitive mutants of calmodulin. *Biochemistry 42*, 2740–2747.
20. Tang, W., Halling, D. B., Black, D. J., Pate, P., Zhang, J. Z., Pedersen, S., Altschuld, R. A., and Hamilton, S. L. (2003) Apocalmodulin and Ca^{2+} calmodulin-binding sites on the Ca(V)1.2 channel. *Biophys. J. 85*, 1538–1547.
21. Black, D. J., Selfridge, J. E., and Persechini, A. (2007) The kinetics of Ca^{2+}-dependent switching in a calmodulin-IQ domain complex. *Biochemistry 46*, 13415–13424.
22. Crivici, A., and Ikura, M. (1995) Molecular and structural basis of target recognition by calmodulin. *Annu. Rev. Biophys. Biomol. Struct. 24*, 85–116.
23. Schuster-Bockler, B., Schultz, J., and Rahmann, S. (2004) HMM logos for visualization of protein families. *BMC Bioinf. 5*, 7.
24. Finn, R. D., Tate, J., Mistry, J., Coggill, P. C., Sammut, S. J., Hotz, H. R., Ceric, G., Forslund, K., Eddy, S. R., Sonnhammer, E. L., and Bateman, A. (2008) The Pfam protein families database. *Nucleic Acids Res. 36*, D281–D288.